TWO-DIMENSIONAL RIEMANN PROBLEM
FOR BURGERS' EQUATION

DAEKI YOON AND WOONJAE HWANG

ABSTRACT. In this paper, we construct the analytic solutions and numerical solutions for a two-dimensional Riemann problem for Burgers' equation. In order to construct the analytic solution, we use the characteristic analysis with the shock and rarefaction base points. We apply the composite scheme suggested by Liska and Wendroff to compute numerical solutions. The result is coincident with our analytic solution. This demonstrates that the composite scheme works pretty well for Burgers' equation despite of its simplicity.

1. Introduction

The Riemann problem in two spatial dimensions for scalar conservation laws is the problem

$$(1) \qquad u_t + f(u)_x + g(u)_y = 0,$$

with initial data that is piecewise constant on a finite number of wedges centered at the origin $x = 0$, $y = 0$. Of particular interest is the four-wedge problem with wedges corresponding to the four quadrants ($\theta_1 = 0, \theta_2 = \pi/2, \theta_3 = \pi, \theta_4 = 3\pi/2$) of the spatial plane, since such initial data is pertinent to numerical finite difference schemes. The typical Riemann data is given in Figure 1.

The study of the two-dimensional Riemann problem was initiated by Guckenheimer [4]. Wagner [14] studied a four-quadrant Riemann problem for the two dimensional single conservation law. Many works for the scalar equation have appeared in [3, 8, 9, 16, 17]. A body of work has been also developed for the system of conservation laws in two dimensions [1, 2, 6, 7, 12, 13, 15, 18].

In section 2, we introduce base points and base curves for rarefaction and shock. We classify the rarefaction and shock as R^+, R^- and S^+, S^-, respectively. We present the composite scheme in section 3. In section 4, we construct
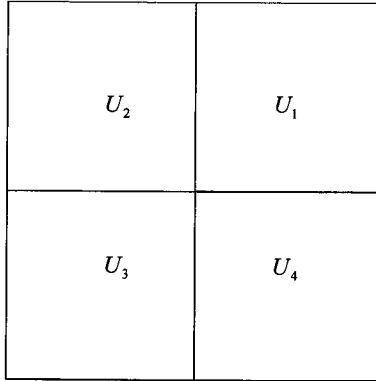
FIGURE 1. Initial condition for Riemann problem

the analytic solutions for two-dimensional Riemann problem for Burgers' equation. We also present numerical solution by the composite scheme to compare it with the analytic solution we construct.

2. Base curve

In this section, we introduce the base point and base curve for shock and rarefaction. These are very important tools for constructing the analytic solution for a two-dimensional Riemann problem. We assume that $f_{uu} \neq 0$, $g_{uu} \neq 0$, and $\partial/\partial u(f_{uu}/g_{uu}) \neq 0$ for any u. This assumption guarantees that the flux functions in any direction have at most one inflection point [17].

2.1. Rarefaction base curves

Under the change of variables $\xi = x/t$, $\eta = y/t$, (1) has the self-similar form

$$(2) \qquad -\xi u_\xi - \eta u_\eta + f(u)_\xi + g(u)_\eta = 0.$$

For $u \in C^1$, (2) becomes

$$(3) \qquad (f_u(u) - \xi)u_\xi + (g_u(u) - \eta)u_\eta = 0$$

whose characteristic form is given by

$$(4) \qquad d\eta(\xi)/d\xi = (g_u(u) - \eta)/(f_u(u) - \xi)$$

and

$$(5) \qquad du(\xi, \eta(\xi))/d\xi = 0.$$

From (4) and (5), the characteristic lines are defined by

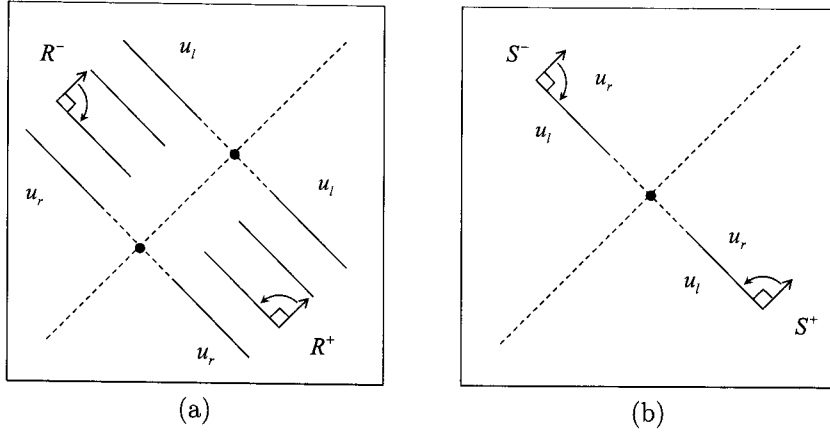$$(6) \qquad \frac{\eta - g_u(u)}{\xi - f_u(u)} = \text{const}, \ u = \text{const}.$$

FIGURE 2. Classification of rarefaction and shock ($u_l > u_r$),
(a) rarefactions R^+, R^-, (b) shocks S^+, S^-

From (6), we note that an u-family level curve with $u = u_0$ is a straight line segment whose tangent passes through the characteristic base point $F_u(u_0)$ in the $\xi\eta$-plane having coordinates

$$(7) \qquad F_u(u_0) \equiv (f_u(u_0), g_u(u_0)).$$

We refer to the curve

$$(8) \qquad F_u(u) \equiv (f_u(u), g_u(u))$$

as the rarefaction base curve. It is easy to show that the rarefaction base curve is monotonic increasing and concave in the $\xi\eta$-plane. Rarefaction waves can be classified according to the direction of the gradient of u across the wave relative to the direction toward the base curve.

Definition ([16]). A rarefaction wave is classified as $R^+(R^-)$ if $\nabla_{\xi,\eta} u$ and the direction toward the base curve of the characteristic lines of the wave form a right- (left-) hand system.

The R^+ and the R^- rarefaction waves are indicated in Figure 2 (a). We note that $u_l > u_r$ in Figure 2.

2.2. Shock base curves

From (2) we have the Rankine-Hugoniot condition for a piecewise smooth shock curve $\eta = \eta(\xi)$,

$$(9) \qquad \frac{d\eta}{d\xi} = \frac{\eta - \sigma^g(u_l, u_r)}{\xi - \sigma^f(u_l, u_r)}$$

where

$$(10) \qquad \sigma^f(u_l, u_r) \equiv \frac{f(u_l) - f(u_r)}{u_l - u_r}, \quad \sigma^g(u_l, u_r) \equiv \frac{g(u_l) - g(u_r)}{u_l - u_r}.$$
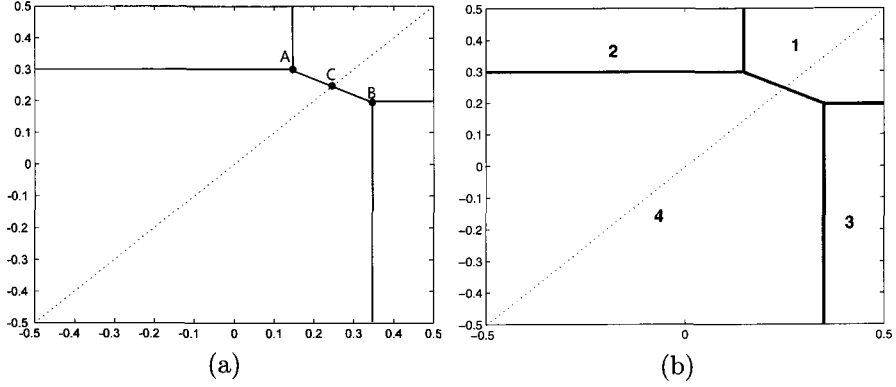
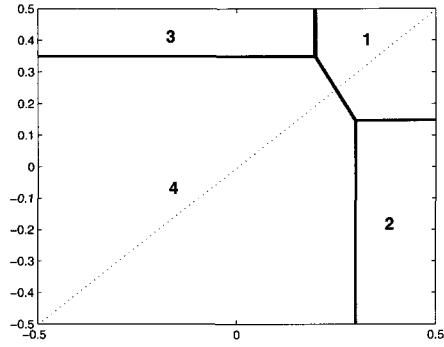FIGURE 3. Four shocks($S^-S^-S^+S^+$)with the initial data (1, 2, 4, 3). (a) analytic solution, (b) numerical solution

FIGURE 4. Four shocks($S^-S^-S^+S^+$) with the initial data (1, 3, 4, 2): numerical solution

From (9) we see that shock point in the $\xi\eta$-plane separating u_l and u_r lies on a curve segment whose tangent at the shock point passes through the shock base point $\sigma(u_l, u_r)$ in the $\xi\eta$-plane having coordinates

$$(11) \qquad \sigma(u_l, u_r) \equiv (\sigma^f(u_l, u_r), \sigma^g(u_l, u_r)).$$

The notation $\sigma(u_l, u_r)$ and $\sigma(u_r, u_l)$ specify the same base point. The curve of base points

$$(12) \qquad \sigma(u, u_r) \equiv (\sigma^f(u, u_r), \sigma^g(u, u_r))$$

denotes the shock base curve for the state u_r. Shock base points are used analogously to rarefaction base points to locally position shocks involving the states u_l and u_r. It is easy to show that shock base curve is monotonic increasing
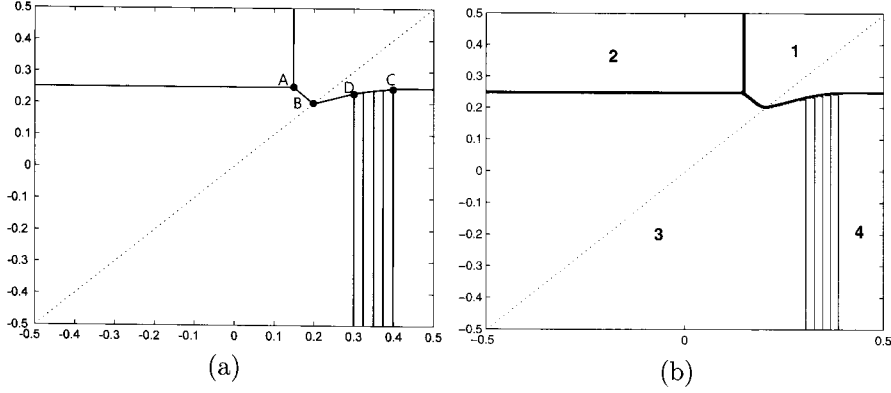
FIGURE 5. Three shocks and one rarefaction$(S^-S^-R^+S^+)$ with the initial data $(1,2,3,4)$. (a) analytic solution, (b) numerical solution

and concave in the $\xi\eta$-plane. A shock wave can be classified according to the relative direction of the shock normal and tangent vectors at each point.

Definition ([16]). A shock wave is classified as $S^+(S^-)$ if at each point the normal and tangent (pointing towards the shock base point) vectors of the shock form a right-hand (left-hand) system.

The S^+ and the S^- shock waves are indicated in Figure 2 (b). The details on base point and base curve can be found in [5, 6, 7, 16].

For $f(u) = g(u)$, the rarefaction and shock base points are located on the straight line $\eta = \xi$.

3. Composite scheme

For the two-dimensional scalar conservation law (1), the first half step of new Lax-Friedrichs(LF) is given by

$$
\begin{aligned}
U_{i+1/2,j+1/2}^{n+1/2} = &\frac{1}{4}[U_{i,j}^n + U_{i+1,j}^n + U_{i,j+1}^n + U_{i+1,j+1}^n] \\
&- \frac{\Delta t}{2\Delta x}[F_{i+1,j+1/2} - F_{i,j+1/2}] \\
&- \frac{\Delta t}{2\Delta y}[G_{i+1/2,j+1} - G_{i+1/2,j}]
\end{aligned}
$$

(13)

where

$$
F_{i+1,j+1/2} = \frac{1}{(\Delta t/2)\Delta y} \int_{y_j}^{y_{j+1}} \int_0^{\Delta t/2} f(\hat{U}(x_{i+1},y,t))dtdy,
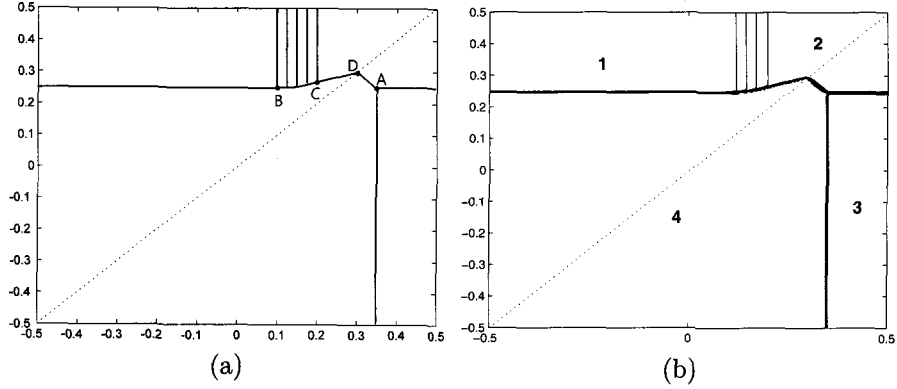$$

FIGURE 6. Three shocks and one rarefaction$(R^-S^-S^+S^+)$ with the initial data $(2,1,4,3)$. (a) analytic solution, (b) numerical solution

and $\hat{U}(x_{i+1}, y, t)$ is the solution, as a function of y and t, of the Riemann problem with initial data

$$\hat{U}(x_{i+1}, y, 0) = \begin{cases} U^n_{i+1,j}, & \text{for } y < y_{j+1/2} \ ; \\ U^n_{i+1,j+1}, & \text{for } y > y_{j+1/2}. \end{cases}$$

Similarly,

$$G_{i+1/2,j+1} = \frac{1}{(\Delta t/2)\Delta x} \int_{x_i}^{x_{i+1}} \int_0^{\Delta t/2} g(\hat{U}(x, y_{j+1}, t)) dt dx,$$

and $\hat{U}(x, y_{j+1}, t)$ is the solution, as a function of x and t, of the Riemann problem with initial data

$$\hat{U}(x, y_{i+1}, 0) = \begin{cases} U^n_{i,j+1}, & \text{for } x < x_{i+1/2} \ ; \\ U^n_{i+1,j+1}, & \text{for } x > x_{i+1/2}. \end{cases}$$

Liska and Wendroff [10, 11] proposed to replace the integrated exact Riemann solutions by a one-dimensional Lax-Friedriechs approximation. The fluxes F and G are evaluated at the LF approximate solution of the 1-D Riemann problems, giving

$$(14) \quad F_{i+1,j+1/2} = f\left(\frac{1}{2}[U^n_{i+1,j+1} + U^n_{i+1,j}] + \frac{\Delta t}{4\Delta y}[g(U^n_{i+1,j+1}) - g(U^n_{i+1,j})]\right),$$

and

$$(15) \quad G_{i+1/2,j+1} = g\left(\frac{1}{2}[U^n_{i+1,j+1} + U^n_{i,j+1}] + \frac{\Delta t}{4\Delta x}[f(U^n_{i+1,j+1}) - f(U^n_{i,j+1})]\right).$$
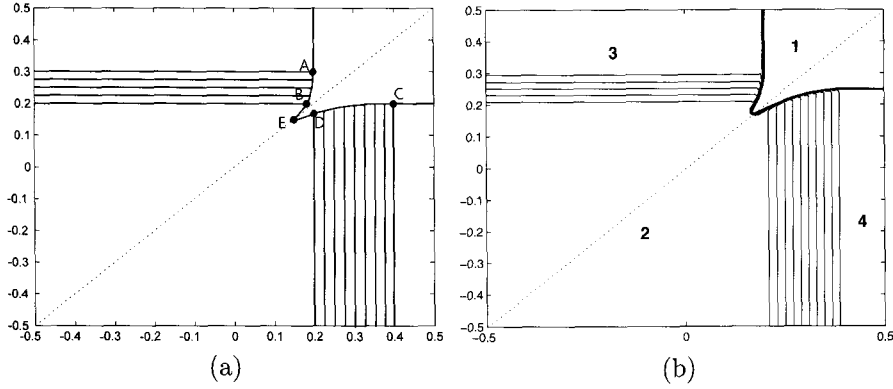
FIGURE 7. Two shocks and two rarefactions$(S^- R^- R^+ S^+)$ with the initial data $(1, 3, 2, 4)$. (a) analytic solution, (b) numerical solution

The second order accurate predictor-corrector scheme is then

$$
\begin{aligned}
U_{i,j}^{n+1} = U_{i,j}^n \\
- \frac{\Delta t}{2\Delta x}\Big[f(U_{i+1/2,j+1/2}^{n+1/2}) + f(U_{i+1/2,j-1/2}^{n+1/2}) \\
- f(U_{i-1/2,j+1/2}^{n+1/2}) - f(U_{i-1/2,j-1/2}^{n+1/2}) \Big] \\
- \frac{\Delta t}{2\Delta y}\Big[g(U_{i+1/2,j+1/2}^{n+1/2}) + g(U_{i-1/2,j+1/2}^{n+1/2}) \\
- g(U_{i+1/2,j-1/2}^{n+1/2}) - g(U_{i-1/2,j-1/2}^{n+1/2}) \Big].
\end{aligned}
$$

(16)

The details can be found in [10, 11]. This second order method is called Corrected Lax-Friedrichs(CF). The idea of the composite scheme is some composition of a second-order method and a first-order method. After applying second-order method for a couple of times, the first-order method is applied to reduce oscillations created by the second-order method. And this process is repeated. We apply $CFLF4$, that is, we apply CF scheme three times and then the LF scheme follows once. Both CF and LF schemes constitute two steps. CF scheme constitutes applying (16) together with (13) and LF scheme constitutes applying (12) twice. The 2-dimensional Burgers' equation is

(17)
$$
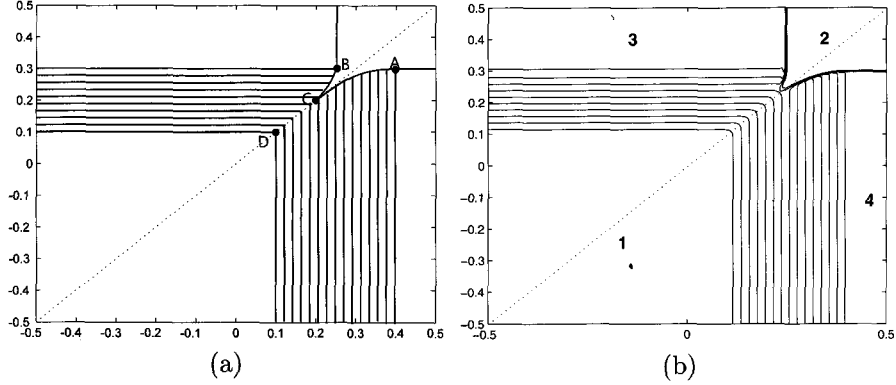u_t + (\frac{1}{2}u^2)_x + (\frac{1}{2}u^2)_y = 0.
$$

FIGURE 8. Two shocks and two rarefactions($S^- R^- R^+ S^+$) with the initial data $(2, 3, 1, 4)$. (a) analytic solution, (b) numerical solution

Since $f(u) = g(u) = \frac{1}{2}u^2$, we have

$$
\begin{aligned}
U^{n+1/2}_{i+1/2,j+1/2} = &\frac{1}{4}[U^n_{i,j} + U^n_{i+1,j} + U^n_{i,j+1} + U^n_{i+1,j+1}] \\
&- \frac{\Delta t}{2\Delta x}[F_{i+1,j+1/2} - F_{i,j+1/2}] \\
&- \frac{\Delta t}{2\Delta y}[G_{i+1/2,j+1} - G_{i+1/2,j}],
\end{aligned}
\tag{18}
$$

$$
F_{i+1,j+1/2} = \frac{1}{2}\left(\frac{1}{2}[U^n_{i+1,j+1} + U^n_{i+1,j}] + \frac{\Delta t}{8\Delta y}[(U^n_{i+1,j+1})^2 - (U^n_{i+1,j})^2]\right)^2,
\tag{19}
$$

$$
G_{i+1/2,j+1} = \frac{1}{2}\left(\frac{1}{2}[U^n_{i+1,j+1} + U^n_{i,j+1}] + \frac{\Delta t}{8\Delta x}[(U^n_{i+1,j+1})^2 - (U^n_{i,j+1})^2]\right)^2,
\tag{20}
$$

and

$$
\begin{aligned}
U^{n+1}_{i,j} = &U^n_{i,j} \\
&- \frac{\Delta t}{4\Delta x}\Big[(U^{n+1/2}_{i+1/2,j+1/2})^2 \\
&+ (U^{n+1/2}_{i+1/2,j-1/2})^2 - (U^{n+1/2}_{i-1/2,j+1/2})^2 - (U^{n+1/2}_{i-1/2,j-1/2})^2\Big] \\
&- \frac{\Delta t}{4\Delta y}\Big[(U^{n+1/2}_{i+1/2,j+1/2})^2 \\
&+ (U^{n+1/2}_{i-1/2,j+1/2})^2 - (U^{n+1/2}_{i+1/2,j-1/2})^2 - (U^{n+1/2}_{i-1/2,j-1/2})^2\Big].
\end{aligned}
\tag{21}
$$

For Burgers' equation, CF scheme constitutes two steps: applying (18) with (19) and (20) and then applying (21). LF scheme also constitutes two steps: applying (18) with (19) and (20) twice.
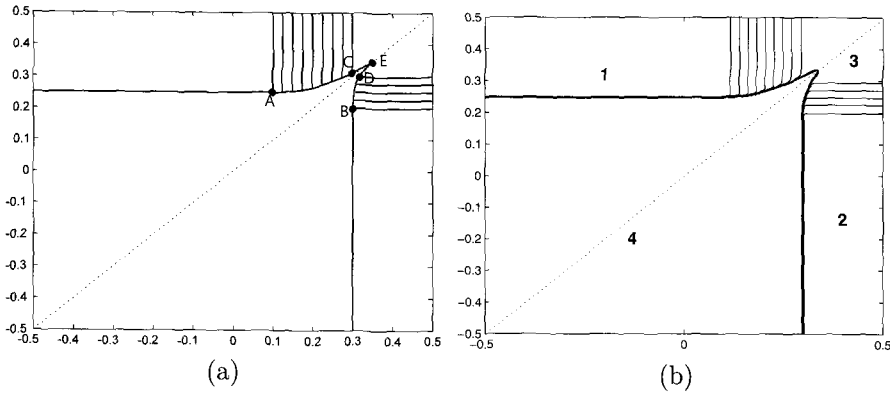
FIGURE 9. Two shocks and two rarefactions$(R^-S^-S^+R^+)$ with the initial data $(3,1,4,2)$. (a) analytic solution, (b) numerical solution

4. Analytic solution and numerical results

We construct the solution for Burgers' equation with the Riemann data: $\{u_1, u_2, u_3, u_4\} = \{1, 2, 3, 4\}$. So we have all $4! = 24$ different cases. The initial data of values $1, 2, 3, 4$ are assigned in each of the four quadrants. The problems are solved on $[-\frac{1}{2}, \frac{1}{2}] \times [-\frac{1}{2}, \frac{1}{2}]$. We use 400×400 uniform meshes. For Burgers equation, the rarefaction base point is (u, u) and the shock base point is $((u_l + u_r)/2, (u_l + u_r)/2)$. We look for the solution at $t = 0.1$. So we scale to $(0.1u, 0.1u)$ and $(0.1(u_l + u_r)/2, 0.1(u_l + u_r)/2)$, respectively. Both rarefaction and shock base curves become $y = x$. To construct the analytic solution, we use the base points given in section 2.

To compute the numerical solution, we apply the composite scheme, $CFLF4$.

4.1. Four shocks

Consider the case $(u_1, u_2, u_3, u_4) = (1, 2, 4, 3)$. In this case, the solution contains only shocks. The S^+ shocks are formed at the initial discontinuities $\theta = 0, \frac{3\pi}{2}$ and the S^- shocks are formed at the initial discontinuities $\theta = \frac{\pi}{2}, \pi$. The S^- shock at $\theta = \frac{\pi}{2}$ is heading for the shock base point $(0.15, 0.15)$ and the S^- shock at $\theta = \pi$ is heading for the shock base point $(0.3, 0.3)$. They meet at the point A. To determine the interaction at the point A, we have to solve the Riemann problem with the Riemann data 1 and 4. As a result, another S^- shock is formed at A and it ends at the shock base point $(0.25, 0.25)$.

On the other hand, the S^+ shock at $\theta = 0$ is heading for the shock base point $(0.2, 0.2)$ and the S^+ shock $\theta = \frac{3\pi}{2}$ is heading for the shock base point $(0.35, 0.35)$. They meet at the point B, where we have to solve another Riemann problem with the Riemann data 4 and 1. Another S^+ shock is formed at B and it ends at the shock base point $(0.25, 0.25)$ and this completes the
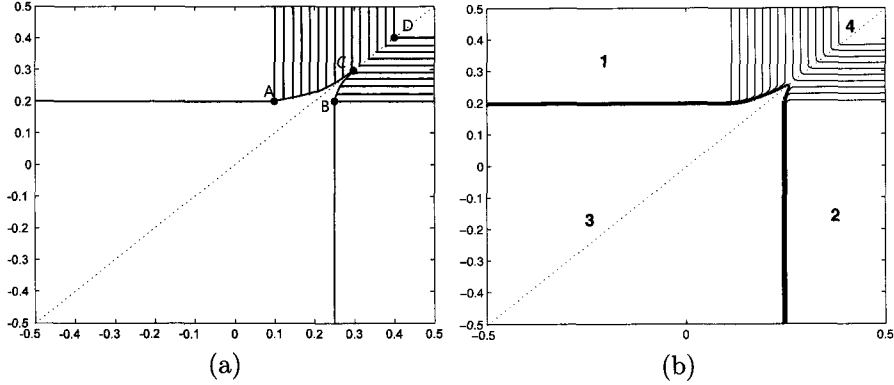
FIGURE 10. Two shocks and two rarefactions$(S^-R^-S^+R^+)$ with the initial data $(4,1,3,2)$. (a) analytic solution, (b) numerical solution

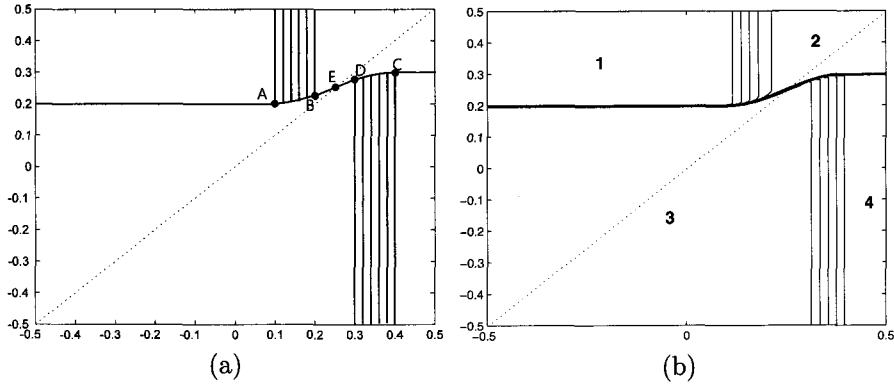

FIGURE 11. Two shocks and two rarefactions$(R^-S^-R^+S^+)$ with the initial data $(2,1,3,4)$. (a) analytic solution, (b) numerical solution

construction of the analytic solution. The analytic solution is given in Figure 3 (a) and numerical solution computed by the composite scheme is given in Figure 3 (b). The case $(u_1, u_2, u_3, u_4) = (1,3,4,2)$ is the inversion of the case $(u_1, u_2, u_3, u_4) = (1,2,4,3)$. If we reflect the Riemann data $(1,3,4,2)$ with respect to the line $y = x$, it gives the exactly same structure of the case $(1,2,4,3)$. The numerical solution with the Riemann data $(1,3,4,2)$ is given in Figure 4. Because of this, we present 12 solutions instead of all 24 solutions.
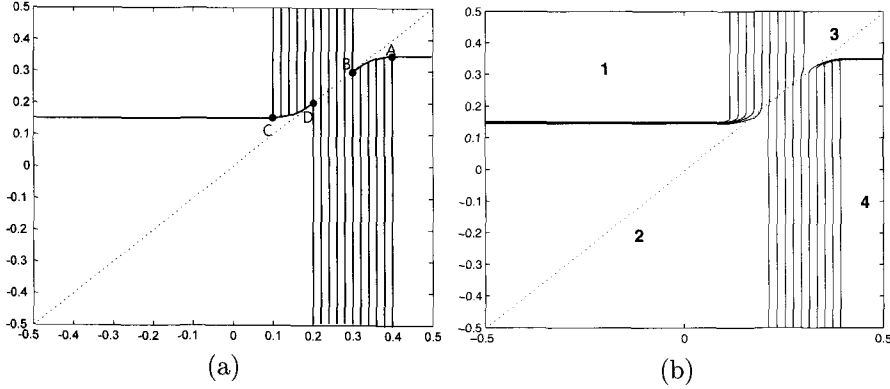
FIGURE 12. Two shocks and two rarefactions$(R^- S^- R^+ S^+)$ with the initial data $(3, 1, 2, 4)$. (a) analytic solution, (b) numerical solution

4.2. Three shocks and one rarefaction

For initial conditions $(u_1, u_2, u_3, u_4) = (1, 2, 3, 4)$, $(1, 4, 3, 2)$, $(2, 1, 4, 3)$, and $(2, 3, 4, 1)$, we have three shocks and one rarefaction. Because of inversion, we consider only $(1, 2, 3, 4)$ and $(2, 1, 4, 3)$ cases. Consider the case $(u_1, u_2, u_3, u_4) = (1, 2, 3, 4)$. In this case, the S^+ shock is formed at the initial discontinuities $\theta = 0$ and the S^- shocks are formed at the initial discontinuities $\theta = \frac{\pi}{2}, \pi$. Two S^- shocks meet at the point A. Another S^- shock is formed at the point A and it ends at the shock base point B $(0.2, 0.2)$. The S^+ shock is heading for the shock base point $(0.25, 0.25)$. The R^+ rarefaction is formed at the initial discontinuities $\theta = \frac{3\pi}{2}$. Left and right ends of rarefaction fan are heading for rarefaction base points $(0.3, 0.3)$ and $(0.4, 0.4)$, respectively. The S^+ shock meets the R^+ rarefaction wave at the point C. The S^+ shock completely penetrates the R^+ rarefaction and at point D we have to solve another Riemann problem with the Riemann data 3 and 1. Another S^+ is formed at point D and it ends at the shock base point B $(0.2, 0.2)$.

From C to D, the S^+ is not a straight shock but a curved shock. It satisfies the ordinary differential equation

$$(22) \qquad \frac{d\eta}{d\xi} = \frac{\eta - \frac{1}{2}(u + 1)}{\xi - \frac{1}{2}(u + 1)}, \quad 3 \le u \le 4,$$

and we can integrate it to find the route of the curved shock. The analytic solution is given in Figure 5 (a) and numerical solution is given in Figure 5 (b).

Similarly, we can construct the analytic solution for the case $(u_1, u_2, u_3, u_4) = (2, 1, 4, 3)$. The analytic and numerical solutions for this case are given in Figure 6 (a) and (b), respectively.
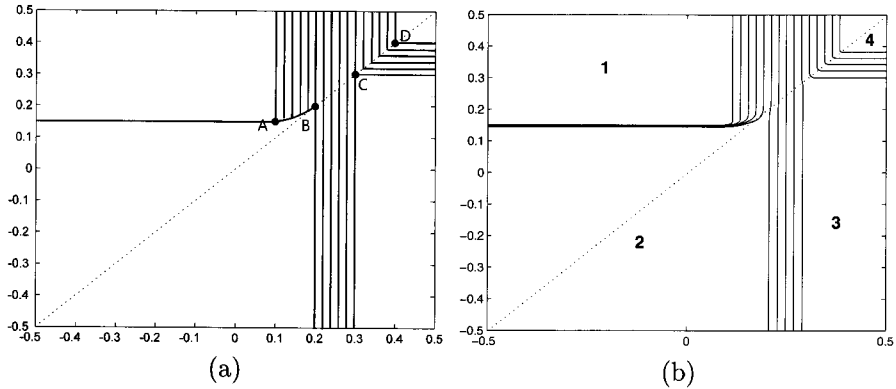
FIGURE 13. One shock and three rarefactions($R^-S^-R^+R^+$) with the initial data $(4, 1, 2, 3)$. (a) analytic solution, (b) numerical solution

4.3. Two shocks and two rarefactions

We have two shocks and two rarefactions for initial conditions (u_1, u_2, u_3, u_4) = $(1, 3, 2, 4)$, $(2, 3, 1, 4)$, $(3, 1, 4, 2)$, $(4, 1, 3, 2)$, $(2, 1, 3, 4)$, and $(3, 1, 2, 4)$. The corresponding inversion cases are $(u_1, u_2, u_3, u_4) = (1, 4, 2, 3)$, $(2, 4, 1, 3)$, $(3, 2, 4, 1)$, $(4, 2, 3, 1)$, $(2, 4, 3, 1)$, and $(3, 4, 2, 1)$, respectively.

Consider the case $(u_1, u_2, u_3, u_4) = (1, 3, 2, 4)$. The S^- shock meets the R^- rarefaction at the point A and it penetrates rarefaction fan completely. At the point B we have to solve the Riemann problem with the Riemann data 1 and 2. The S^- shock is formed at the point B and it ends at the shock base point E $(0.15, 0.15)$. The S^+ shock interacts the R^+ rarefaction at the point C and it penetrates rarefaction fan completely. At the point D we again have to solve the Riemann problem with the Riemann data 2 and 1. The S^+ shock is formed at the point D and it ends at the shock base point E $(0.15, 0.15)$. The analytic solution is given in Figure 7 (a) and numerical solution is given in Figure 7 (b).

For the cases $(u_1, u_2, u_3, u_4) = (2, 3, 1, 4)$ and $(3, 1, 4, 2)$ we can construct the analytic solution similarly. The analytic and numerical solutions for these cases are given in Figure 8 and 9, respectively.

Consider the case $(u_1, u_2, u_3, u_4) = (4, 1, 3, 2)$. The R^- rarefaction meets the S^- shock at the point A and the R^+ rarefaction at the rarefaction base point D $(0.4, 0.4)$. The S^- shock becomes a curved shock at the point A and it ends at the point C $(0.3, 0.3)$. The S^+ shock begins interaction at the point B with the R^+ rarefaction and it terminates with a zero strength at the point C. The analytic solution is given in Figure 10 (a) and numerical solution is given in Figure 10 (b).
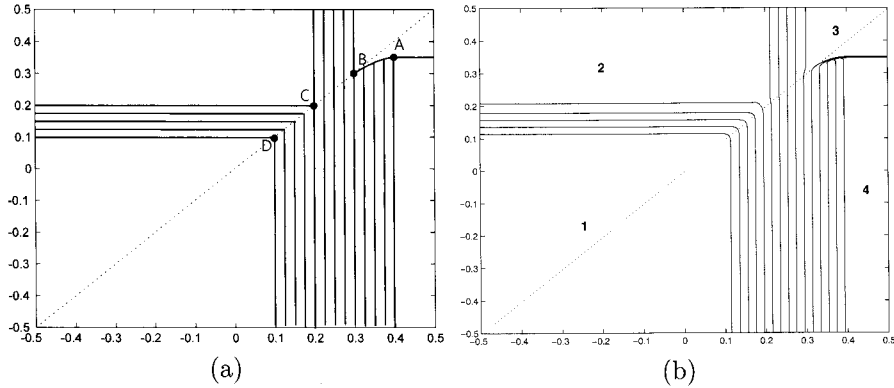
(a)   (b)

FIGURE 14. One shock and three rarefactions$(R^-R^-R^+S^+)$ with the initial data $(3,2,1,4)$. (a) analytic solution, (b) numerical solution

Consider the case $(u_1, u_2, u_3, u_4) = (2, 1, 3, 4)$. The S^- shock meets the R^- rarefaction at the point A. The S^- shock penetrates the R^- rarefaction fan completely and we have to solve the Riemann problem at the point B with the Riemann data 2 and 3. As a result, the S^- shock is formed at the point B and it ends at the shock base point E $(0.25, 0.25)$. The S^+ shock penetrates the R^+ rarefaction fan completely and the S^+ shock is formed at the point D and it ends at the shock base point E. The analytic solution is given in Figure 11 (a) and numerical solution is given in Figure 11 (b).

For the case $(u_1, u_2, u_3, u_4) = (3, 1, 2, 4)$, we can construct the analytic solution similarly. The analytic solution is given in Figure 12 (a) and numerical solution is given in Figure 12 (b).

4.4. One shock and three rarefactions

We have one shock and three rarefactions for initial conditions (u_1, u_2, u_3, u_4) $= (4, 1, 2, 3), (4, 3, 2, 1), (3, 2, 1, 4), (3, 4, 1, 2)$. Because of inversion, we consider only $(4, 1, 2, 3)$ and $(3, 2, 1, 4)$ cases.

The S^- shock meets the R^- rarefaction at the point A and it terminates with a zero strength at the point B $(0.2, 0.2)$. The R^+ rarefaction is formed at the initial discontinuity $\theta = \frac{3\pi}{2}$. Left and right ends of the rarefaction fan are heading for the rarefaction base points B $(0.2, 0.2)$ and C $(0.3, 0.3)$, respectively. Another R^+ rarefaction is formed at the initial discontinuity $\theta = 0$. Left and right ends of the rarefaction fan are heading for the rarefaction base points C $(0.3, 0.3)$ and D $(0.4, 0.4)$, respectively. The analytic solution is given in Figure 13 (a) and numerical solution is given in Figure 13 (b).

Similarly, we can construct the analytic solution for the case (u_1, u_2, u_3, u_4) $= (3, 2, 1, 4)$. The analytic solution is given in Figure 14 (a) and numerical solution is given in Figure 14 (b).
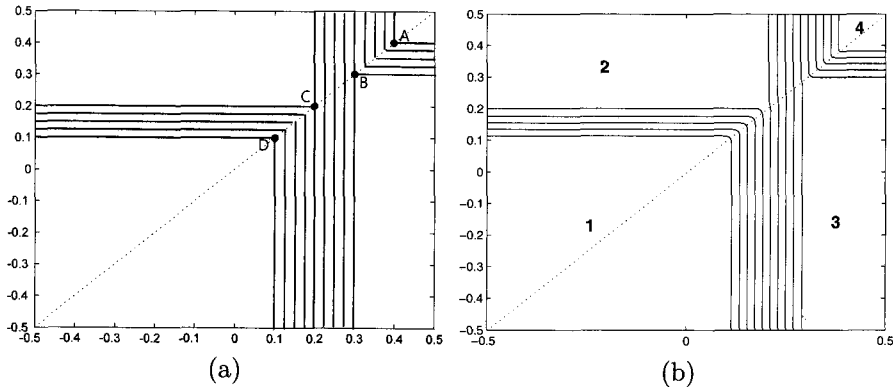
FIGURE 15. Four rarefactions($R^-R^-R^+R^+$) with the initial data $(4, 2, 1, 3)$. (a) analytic solution, (b) numerical solution

4.5. Four rarefactions

For initial conditions $(u_1, u_2, u_3, u_4) = (4, 2, 1, 3), (4, 3, 1, 2)$, we have all four rarefactions. Because of inversion, we consider only $(4, 2, 1, 3)$ case.

The R^- and the R^+ interact at the rarefaction base point A $(0.4, 0.4)$. Two R^+ meet at the rarefaction base point B $(0.3, 0.3)$. Again the R^- and the R^+ interact at the rarefaction base point D $(0.1, 0.1)$. Two R^- meet at the rarefaction base point C $(0.2, 0.2)$. The analytic solution is given in Figure 15 (a) and numerical solution is given in Figure 15 (b).

References

[1] T. Chang, G. Chen, and S. Yang, *On the 2-D Riemann problem for the compressible Euler equations. I. Interaction of shocks and rarefaction waves*, Discrete Contin. Dynam. Systems **1** (1995), no. 4, 555–584.

[2] T. Chang and L. Hsiao, *The Riemann Problem and Interaction of Waves in Gas Dynamics*, Pitman Monographs and Surveys in Pure and Applied Mathematics, 41. Longman Scientific & Technical, Harlow; copublished in the United States with John Wiley & Sons, Inc., New York, 1989.

[3] G. Chen, D. Li, and D. Tan, *Structure of Riemann solutions for 2-dimensional scalar conservation laws*, J. Differential Equations **127** (1996), no. 1, 124–147.

[4] J. Guckenheimer, *Shocks and rarefactions in two space dimensions*, Arch. Rational Mech. Anal. **59** (1975), no. 3, 281–291.

[5] W. Hwang, *The 2-dimensional Riemann problem*, J. Inst. Sci. Tech. Korea University **12** (2004), 29–34.

[6] W. Hwang and W. B. Lindquist, *The 2-dimensional Riemann problem for a 2 × 2 hyperbolic conservation law. I. Isotropic media*, SIAM J. Math. Anal. **34** (2002), no. 2, 341–358.

[7] ———, *The 2-dimensional Riemann problem for a 2 × 2 hyperbolic conservation law. II. Anisotropic media*, SIAM J. Math. Anal. **34** (2002), no. 2, 359–384.

[8] W. B. Lindquist, *The scalar Riemann problem in two spatial dimensions: piecewise smoothness of solutions and its breakdown*, SIAM J. Math. Anal. **17** (1986), no. 5, 1178–1197.

[9] ———, *Construction of solutions for two-dimensional Riemann problems*, Hyperbolic partial differential equations, III. Comput. Math. Appl. Part A **12** (1986), no. 4-5, 615–630.

[10] R. Liska and B. Wendroff, *Composite schemes for conservation laws*, SIAM J. Numer. Anal. **35** (1998), no. 6, 2250–2271.

[11] ———, *Two dimensional shallow water equations by composite schemes*, Int. J. Numer. Meth. Fluids **30** (1999), 461–479.

[12] C. Schulz-Rinne, *Classification of the Riemann problem for two-dimensional gas dynamics*, SIAM J. Math. Anal. **24** (1993), no. 1, 76–88.

[13] C. Schulz-Rinne, J. Collins, and H. Glaz, *Numerical solution of the Riemann problem for two-dimensional gas dynamics*, SIAM J. Sci. Comput. **14** (1993), no. 6, 1394–1414.

[14] D. Wagner, *The Riemann problem in two space dimensions for a single conservation law*, SIAM J. Math. Anal. **14** (1983), no. 3, 534–559.

[15] T. Zhang and G. Chen, *Some fundamental concepts about system of two spatial dimensional conservation laws*, Acta Math. Sci. (English Ed.) **6** (1986), no. 4, 463–474.

[16] P. Zhang and T. Zhang, *Generalized characteristic analysis and Guckenheimer structure*, J. Differential Equations **152** (1999), no. 2, 409–430.

[17] T. Zhang and Y. Zheng, *Two-dimensional Riemann problem for a single conservation law*, Trans. Amer. Math. Soc. **312** (1989), no. 2, 589–619.

[18] ———, *Conjecture on the structure of solutions of the Riemann problem for two-dimensional gas dynamics systems*, SIAM J. Math. Anal. **21** (1990), no. 3, 593–630.

DAEKI YOON
DEPARTMENT OF MATHEMATICS
KOREA UNIVERSITY
SEOUL 136-701, KOREA
E-mail address: dyoon@korea.ac.kr

WOONJAE HWANG
DEPARTMENT OF INFORMATION AND MATHEMATICS
KOREA UNIVERSITY
JOCHIWON 739-700, KOREA
E-mail address: woonjae@korea.ac.kr